

GigaScience

Chromosome-level genome assembly of the hard-shelled mussel *Mytilus coruscus*, a widely distributed species from the temperate areas of East Asia --Manuscript Draft--

Manuscript Number:	GIGA-D-20-00287R2	
Full Title:	Chromosome-level genome assembly of the hard-shelled mussel <i>Mytilus coruscus</i> , a widely distributed species from the temperate areas of East Asia	
Article Type:	Data Note	
Funding Information:	the National Key Research and Development Program of China (2018YFD0900601)	Doctoral Yi-Feng Li
	International Science and Technology Cooperation Programme (CN) (2018YFD0900101)	Professor Ying Lu
	the National Natural Science Foundation of China (41876159)	Professor Jin-Long Yang
	the National Natural Science Foundation of China (41606147)	Doctoral Xiao Liang
	the National Natural Science Foundation of China (31802321)	Doctoral Yi-Feng Li
	Guangdong Key Laboratory of Fermentation and Enzyme Engineering (CN) (GML2019ZD0402)	Professor Jin-Long Yang
	the Shanghai Sailing Program (18YF1410000)	Doctoral Yi-Feng Li
	Program for study on genetic resources, environment and strategy of mussel culture in coast of Gouqi Island offshore	Professor Jin-Long Yang
	China Postdoctoral Science Foundation (2019M6614770)	Doctoral Dan-Dan Feng
Abstract:	<p>Background: The hard-shelled mussel (<i>Mytilus coruscus</i>) is widely distributed in the temperate seas of East Asia, and is an important commercial bivalve in China. Chromosome-level genome information of this species will not only contribute to the development of hard-shelled mussel genetic breeding, but also to studies on larval ecology, climate change biology, marine biology, aquaculture, biofouling, and antifouling. Findings: We applied a combination of Illumina sequencing, Oxford Nanopore Technologies sequencing, and high-throughput chromosome conformation capture technologies to construct a chromosome-level genome of the hard-shelled mussel, with a total length of 1.57 Gb and a median contig length of 1.49 Mb. Approximately 90.9% of the assemblies were anchored to 14 linkage groups. Comparison to the Core Eukaryotic Genes Mapping Approach (CEGMA) metazoan complement revealed that the genome possesses 91.9% of core metazoan orthologs. Gene modeling enabled the annotation of 37,478 protein-coding genes and 26,917 non-coding RNA loci. Phylogenetic analysis showed that <i>M. coruscus</i> is the sister taxon to the clade including <i>Modiolus philippinarum</i> and <i>Bathymodiolus platifrons</i>. Conserved chromosome synteny was observed between hard-shelled mussel and king scallop, suggesting that this is shared ancestrally. Transcriptomic profiling indicated that the pathways of catecholamine biosynthesis and adrenergic signaling in cardiomyocytes might be involved in metamorphosis. Conclusions: The chromosome-level assembly of the hard-shelled mussel genome will provide novel insights into mussel genome evolution and serve as a fundamental platform for studies regarding the planktonic-sessile transition, genetic diversity, and genomic breeding of this bivalve.</p>	
Corresponding Author:	Ying Lu Shanghai Ocean University Shanghai, CHINA	

Corresponding Author Secondary Information:	
Corresponding Author's Institution:	Shanghai Ocean University
Corresponding Author's Secondary Institution:	
First Author:	Jin-Long Yang
First Author Secondary Information:	
Order of Authors:	Jin-Long Yang
	Dan-Dan Feng
	Jie Liu
	Jia-Kang Xu
	Ke Chen
	Yi-Feng Li
	You-Ting Zhu
	Xiao Liang
	Ying Lu
Order of Authors Secondary Information:	
Response to Reviewers:	<p>GIGA-D-20-00287R2.</p> <p>Dear Dr. Hans Zauner Giga Science</p> <p>Thank you so much for your time and valuable help in improving the manuscript. Please find below our detailed responses addressing the comments (answers in blue).</p> <p>Reviewer Comments: Reviewer #2: The response by Yang et al has mostly addressed my concerns. However, I have a few remaining points to address, which should be corrected before acceptance. Major points to address: 1) the main text tables have not been provided, and I am unable to assess their contents. I do not need to see these again provided the editor can confirm their veracity. in answer to my major point 1) regarding N content as I cannot see if this information is provided in the table, please ensure that it is noted either in the main text or in the table legend that gaps are preset at 100Ns, and may be longer or shorter. It may be useful to give a "total number of gaps" figure in this table. Yes, total numbers of gaps are listed in Table 2 of the revision, which describes that each gap is preset at 100 Ns (Line 675-676).</p> <p>2) for Figure 5 it is still confusing why <i>M. coruscus</i> is not compared to all the other genomes, rather than doing these comparisons with another species (which has been studied previously). Would you like to show more <i>M. coruscus</i> results? Thanks for your suggestion. We construct the synteny between <i>M. coruscus</i> and four reported chromosome-level genomes in the revision (Fig. 5). In the main text (Fig.5), <i>P. maximus</i> is selected as a reference to illustrate gene collinearity (<i>P. maximus</i> vs another 4 species, including <i>M. coruscus</i>) due to its slow evolution. The synteny between the hard-shelled mussel and another three species (Pacific oyster, blood clam, pearl oyster) is added in the Fig. 5g-h of the revision (mentioned in main text Line 309-312, Line 475-478) as the follows: In addition, the high gene collinearity between the hard-shelled mussel and another three bivalves of the Pacific oyster, blood clam and pearl oyster also reflected the satisfied quality of the hard-shelled mussel assemblies (Fig. 5f-h).</p> <p>Figure 5. Chromosome synteny. a. Alignment of king scallop and blood clam</p>

chromosomes. b. Alignment of king scallop and hard-shelled mussel chromosomes. c. Alignment of king scallop and pearl oyster chromosomes. d. Alignment of king scallop and Pacific oyster chromosomes. e. Rearrangements between the chromosomes of king scallop and those of four other bivalve species. The king scallop chromosomes are represented by bars of different colors, and synteny and rearrangements in the chromosomes of the four other bivalves are indicated by different blocks, whose colors correspond to those of the reference king scallop chromosomes, the dashed lines indicate the corresponding evolutionary relationship. f. Alignment of hard-shelled mussel and blood clam chromosomes. g. Alignment of hard-shelled mussel and pearl oyster chromosomes. h. Alignment of hard-shelled mussel and Pacific oyster chromosomes. The king scallop linkage groups are labeled as PM 1 to 19, the blood clam chromosomes as SB 1 to 19, the hard-shelled mussel chromosomes as MC 1 to 14, the pearl oyster chromosomes as PF 1 to 14, and the Pacific oyster chromosomes as CG 1 to 10. Scale unit, Mb. a-d, f-h. The circularized blocks represent the chromosomes of the five bivalves. Aligned homologous genes are connected by ribbons, shown in different colors depending on their chromosome location.

3) in Fig 6b, please indicate in the figure legend whether these results are the averages of your 3 replicate samples, or individual samples
Thanks for your suggestion. We describe the information in the legend of the Fig. 6b that these quantification results of gene expression are the averages of three replicate samples. (Line 495-496).

Minor points:

The manuscript would still benefit from another round of proof reading. I have noted some problems below.

Thanks for your suggestion, we have performed another round of proof reading.

Abstract:

-Linkage misspelled, "14 lineage groups"

Sorry for the typo. The misspelling is corrected in the revision (Line 30).

-carried is the wrong word, and the past tense is incorrect here: "carried 91.9% of core metazoan orthologs." Perhaps "possesses 91.9% of the core metazoan ortholog set"
Sorry for the confusion. The sentence is corrected as "the genome possesses 91.9% of the core metazoan ortholog set" (Line 32).

- "the sister taxon" not "a sister taxon" (also in methods section)

Sorry for the mistake. We replace "a sister taxon" by "the sister taxon" in both abstract and method sections (Line 34 and Line 247).

Introduction:

- "due to their high economic" not "due to the high"

Sorry. We have corrected it in the revision. (Line 48).

- "understanding of the larvae-juvenile" not "understanding of larvae-juvenile"

Sorry for the mistake. We correct it in the revision (Line 64).

- "widespread among metazoans" not "widespread among metazoan "

Sorry for the mistake. We correct it in the revision (Line 68).

- "Most studies" not "Most of studies"

Sorry for the mistake. "of " is removed from that phrase (Line 74).

- "hard-shelled mussel genetic breeding" not "the hard-shelled mussel genetic breeding" (no the)

Sorry for the mistake. "the " is removed from that sentence in the revision (Line 80).

- I suggest "molluscs" rather than "mollusks" in the last paragraph, to match your usage elsewhere

Thanks for your suggestion, "mollusks" is replaced by "molluscs" (Line 88 and Line 375).

	<p>Methods:</p> <p>- no "a"s in "at a 57× coverage and the heterozygous peak was at a 28×" - this should read "at 57× coverage and the heterozygous peak was at 28×" Sorry for the mistake. "a" is removed from "at a 57× coverage and the heterozygous peak was at a 28×" in the revision (Line 152-153).</p> <p>-"usually occurs in fragmented assemblies" not "usually occurs in fragmented assembly", Sorry for the mistake. We correct it in the revision (Line 158).</p> <p>-"align to one or more of the InterPro " not "have the alignment to one or more of the InterPro" Thanks. The sentence is corrected as "35,471 protein-coding genes (94.6% of the 37,478 gene models) align to one or more of the InterPro " (Line 218).</p> <p>-"Chromosome-level genomes allow re-sequencing and population genetic studies." not "Chromosome-level genome is important for re-sequencing and population genetic." As your suggestions, the sentence is corrected as "Chromosome-level genomes allow re-sequencing and population genetic studies" (Line 251).</p> <p>-"preliminary assay" not "preliminary try " Thanks for your suggestions. We use "assay", instead (Line 252).</p> <p>-"Benchmark Universal Single-Copy Orthologs (BUSCO) v4.1.4" not "Benchmark Universal Single-Copy Orthologs BUSCO v4.1.4" As your suggestion, "Benchmark Universal Single-Copy Orthologs BUSCO v4.1.4" is replaced by "Benchmark Universal Single-Copy Orthologs (BUSCO) v4.1.4" (Line 354).</p> <p>Abbreviations" no "the", TPM: Transcripts per Million; As your suggestion, "the" is removed (Line 388).</p> <p>Figure 3 legend (and possibly elsewhere) please italicise the k in kmer As your suggestion, we italicize the k in k-mer (Line 148-153, Line 587, Line 593).</p> <p>Figure 4 legend: gene names need italics Thanks for your suggestion. We italicize the gene names as chitobiase (Line 460-461).</p> <p>Fig 5 legend: "corresponding evolutionary relationship" not "corresponding evolution relationship" Thanks for your suggestion. We correct it in the revision (Line 475).</p> <p>-some bold font needed, Additional Files title page (pg 25) Thanks for your suggestion. Bold font is used in the revision (Line 513, Line 515).</p>
Additional Information:	
Question	Response
Are you submitting this manuscript to a special series or article collection?	No
Experimental design and statistics	Yes
Full details of the experimental design and statistical methods used should be given in the Methods section, as detailed in our Minimum Standards Reporting Checklist . Information essential to interpreting the	

<p>data presented should be made available in the figure legends.</p> <p>Have you included all the information requested in your manuscript?</p>	
<p>Resources</p> <p>A description of all resources used, including antibodies, cell lines, animals and software tools, with enough information to allow them to be uniquely identified, should be included in the Methods section. Authors are strongly encouraged to cite Research Resource Identifiers (RRIDs) for antibodies, model organisms and tools, where possible.</p> <p>Have you included the information requested as detailed in our Minimum Standards Reporting Checklist?</p>	<p>Yes</p>
<p>Availability of data and materials</p> <p>All datasets and code on which the conclusions of the paper rely must be either included in your submission or deposited in publicly available repositories (where available and ethically appropriate), referencing such data using a unique identifier in the references and in the “Availability of Data and Materials” section of your manuscript.</p> <p>Have you have met the above requirement as detailed in our Minimum Standards Reporting Checklist?</p>	<p>Yes</p>

1 **Chromosome-level genome assembly of the hard-shelled mussel**
2 ***Mytilus coruscus*, a widely distributed species from the temperate**
3 **areas of East Asia**

4 Jin-Long Yang^{1,2,3,†,*}, Dan-Dan Feng^{1,2,†}, Jie Liu^{1,2,†}, Jia-Kang Xu^{1,2}, Ke Chen^{1,2}, Yi-
5 Feng Li^{1,2}, You-Ting Zhu^{1,2}, Xiao Liang^{1,2}, Ying Lu^{1,2}, ORCID: [0000-0002-2509-9209](https://orcid.org/0000-0002-2509-9209)*

6 ¹ International Research Center for Marine Biosciences, Ministry of Science and
7 Technology, Shanghai Ocean University, Shanghai, China

8 ² Key Laboratory of Exploration and Utilization of Aquatic Genetic Resources,
9 Ministry of Education, Shanghai Ocean University, Shanghai, China

10 ³ Southern Marine Science and Engineering Guangdong Laboratory, Guangzhou, China

11

12 † These authors contributed equally: Jin-Long Yang, Dan-Dan Feng, Jie Liu.

13 * Corresponding author. E-mail: jlyang@shou.edu.cn, yinglu@shou.edu.cn

14 Tel: + 86-21-61900403; Fax: + 86-21-61900405

15

16

17

18

19

20 **Abstract**

21 **Background:** The hard-shelled mussel (*Mytilus coruscus*) is widely distributed in the
22 temperate seas of East Asia, and is an important commercial bivalve in China.
23 Chromosome-level genome information of this species will not only contribute to the
24 development of hard-shelled mussel genetic breeding, but also to studies on larval
25 ecology, climate change biology, marine biology, aquaculture, biofouling, and
26 antifouling. **Findings:** We applied a combination of Illumina sequencing, Oxford
27 Nanopore Technologies sequencing, and high-throughput chromosome conformation
28 capture technologies to construct a chromosome-level genome of the hard-shelled
29 mussel, with a total length of 1.57 Gb and a median contig length of 1.49 Mb.
30 Approximately 90.9% of the assemblies were anchored to 14 linkage groups. We
31 assayed the genome completeness using Benchmark Universal Single-Copy Orthologs
32 (BUSCO). In the metazoan dataset, the current assemblies have 89.4% complete, 1.9%
33 incomplete and 8.7% missing BUSCOs. Gene modeling enabled the annotation of
34 37,478 protein-coding genes and 26,917 non-coding RNA loci. Phylogenetic analysis
35 showed that *M. coruscus* is the sister taxon to the clade including *Modiolus*
36 *philippinarum* and *Bathymodiolus platifrons*. Conserved chromosome synteny was
37 observed between hard-shelled mussel and king scallop, suggesting that this is shared
38 ancestrally. Transcriptomic profiling indicated that the pathways of catecholamine
39 biosynthesis and adrenergic signaling in cardiomyocytes might be involved in
40 metamorphosis. **Conclusions:** The chromosome-level assembly of the hard-shelled
41 mussel genome will provide novel insights into mussel genome evolution and serve as

42 a fundamental platform for studies regarding the planktonic-sessile transition, genetic
43 diversity, and genomic breeding of this bivalve.

44 *Keywords: Mytilus coruscus, genome sequencing, Hi-C, chromosome, metamorphosis*

45

46 **Context**

47 Marine mussels, which belong to the phylum Mollusca, settle on most immersed
48 surfaces of substrata and play a crucial role in marine ecosystems. As healthy and
49 sustainable food items, these mussels are beneficial for humans due to their high
50 economic value for fishery and aquaculture, constituting more than 8% of mollusc
51 aquaculture production [1]. Simultaneously, mussels are also known as typical
52 macrofouling organisms that result in detrimental economic and ecological
53 consequences for the maritime and aquaculture industries [2-4]. Mussels have been
54 used as model organisms for adaptation to climate change, biomonitoring, integrative
55 ecomechanics, biomaterials, larval ecology, settlement and metamorphosis, adhesion,
56 bacteria-host interaction, biofouling and antifouling studies [5-12]. Although they are
57 significant for biology, ecology and the economy, whole genome information of marine
58 mussels is limited [13, 14] and this lack of knowledge postpones our understanding the
59 molecular basis of adaption, evolution, breeding, genetic manipulation, bacteria-host
60 interaction, and settlement mechanism.

61 As many other marine invertebrates, marine mussels also possess a free-swimming
62 larval phase. After this stage, these minute larvae will settle on the substrata and finish
63 metamorphosis transition, accompanied with dramatic remodeling of their anatomy [4,

64 15]. Multiple physicochemical stimuli play critical roles in the process of larval
65 settlement and metamorphosis [15-17]. Thus, understanding of the larvae-juvenile
66 transition process is still a keystone question in marine biology, larval ecology,
67 aquaculture, biofouling and antifouling [4, 15, 18, 19]. The finding that chemical cues
68 from bacterial biofilms trigger settlement and metamorphosis is widespread among
69 metazoans [15, 16, 18].

70 The hard-shelled mussel (*Mytilus coruscus* Gould 1861, NCBI Taxonomy ID:
71 42192, **Fig. 1**) mainly inhabits temperate areas along the coastal waters of China, Japan,
72 Korea and Far East of Russia, covering from East China Sea to Sea of Japan [20]. In
73 China, the hard-shelled mussel is an important commercial bivalve as well as a typical
74 macrofouling organism. As a sessile marine bivalve, the hard-shelled mussel needs to
75 adapt to the hostile and complex environments of intertidal regions. Most studies
76 focused on the planktonic-sessile transition mechanism of receptor and biofilm
77 regulation, host-bacteria interaction, aquaculture and biofouling and antifouling studies
78 in this species [3-5, 12, 21-23]. To date, no genome of any member of the genus *Mytilus*
79 has been assembled at the chromosome level, although a draft genome of *M. coruscus*
80 [24] and an improved genome of *M. galloprovincialis* [13, 25] have been reported. The
81 lack of whole-genome information has hindered the development of hard-shelled
82 mussel genetic breeding, larval ecology, climate change biology, marine biology,
83 aquaculture, biofouling and antifouling studies.

84 In this study, we report a chromosome-level assembly of the hard-shelled mussel
85 genome obtained by combining Illumina sequencing, Oxford Nanopore Technologies

86 (ONT) sequencing, and high-throughput chromosome conformation capture (Hi-C)
87 technologies. We validated the genome assemblies by chromosome synteny analysis,
88 comparing them with the published chromosome-level genomes of the most studied
89 molluscs. Larvae at five early developmental stages were subjected to RNA sequencing
90 (RNA-seq) analysis for the profiling of gene expression during metamorphosis.
91 Accessible chromosome-level genome datasets [26, 27] will facilitate comparative
92 genomics studies on chromosome rearrangements across different species.

93

94 **Methods**

95 **Sample information and collection**

96 Wild individuals for genome sequencing were collected from the coast of Shengsi,
97 Zhejiang province, which is the central coast of the Chinese mainland, and one of the
98 original and main breeding areas of the hard-shelled mussel in China. Farmed and wild
99 adults were also collected from the coast of Shengsi (122.77E 30.73N and 122.74E
100 30.71N, respectively) (**Fig. 1**). A female wild adult with a mature ovary was dissected,
101 and the adductor muscle was collected to isolate high-molecular-weight genomic DNA
102 for the sequencing of the reference genome. The DNA extracted from the farmed and
103 wild populations (10 individuals per population) was pooled for genome re-sequencing.
104 Adductor muscle, mantle, gill, digestive gland, hemocyte, labial palp, female gonad,
105 male gonad, foot, and gut tissues were dissected from fresh samples for transcriptome
106 sequencing to assist with the prediction of protein-coding genes.

107

108 **Isolation of genomic DNA and RNA**

109 Genomic DNA was extracted from fresh adductor muscle tissue using the SDS
110 extraction method [28], and then used for sequencing on an ONT PromethION platform
111 (Oxford Nanopore Technologies, UK). Using the TIANamp Marine Animals DNA kit
112 (Tiangen, China), DNA for whole genome re-sequencing was extracted from the
113 muscles of five female and five male individuals from each population. Using the
114 RNAiso Plus kit (TaKaRa, Japan), total RNA was extracted from 10 different tissues of
115 five female and five male individuals from each population to obtain a large gene
116 expression dataset. Fresh muscle cells were crosslinked with formaldehyde, and
117 digestion, marking of DNA ends, and blunt-end ligation were performed as described
118 in a previous study [29]. The purified DNA was used for Hi-C.

119

120 **Genome sequencing with different technologies**

121 A combined sequencing strategy was applied to obtain the hard-shelled mussel genome
122 (**Fig. 2**). Qualified DNA was filtered using a BluePippin™ System to extract large
123 fragments. The large-fragment DNA was employed to construct a library using the ONT
124 Template prep kit and the NEB Next FFPE DNA Repair Mix kit [New England Biolabs
125 (NEB), USA]. A high-quality library with an average length of 20 kb was sequenced
126 on the ONT PromethION platform with the corresponding R9 cell and ONT sequencing
127 reagent kit. A total of 246.8 Gb of data (~159× coverage) were generated (**Table 1**).

128 Sequencing of Hi-C and genome survey libraries was performed on an Illumina
129 sequencing platform. Briefly, the extracted DNA was fragmented to a size of 300–350

130 bp using an E210 Focused Ultrasonicator (Covaris, USA). The construction of paired-
131 end libraries encompassed the successive steps of end repair, poly(A) addition, barcode
132 indexing, purification, and PCR amplification. The libraries were sequenced with the
133 Illumina NovaSeq 6000 platform (Illumina, USA) to generate 150-bp paired-end reads.
134 Sequencing of the Hi-C libraries generated a total of 249.6 Gb of data (~161× coverage),
135 and sequencing of the genome survey libraries generated a total of 160.6 Gb of data
136 (~104× coverage).

137 The qualified RNA extracted from the same tissues of 10 individuals was equally
138 mixed for RNA-seq. The sample was enriched in mRNA by extracting poly(A)
139 transcripts from total RNA using oligo-d(T) magnetic beads. Sequencing libraries were
140 prepared using the NEBNext® Ultra™ RNA Library Prep Kit for Illumina® (NEB,
141 USA) following the manufacturer's recommendations. A total of 10 libraries were
142 sequenced on the Illumina NovaSeq 6000 platform in a 150-bp paired-end mode.

143 The raw reads from Illumina sequencing platform were cleaned using FastQC45 and
144 HTQC46 by the following steps: (a) filtered reads with adapter sequence; (b) filtered
145 PE reads with one reads more than 10% N bases; (c) filtered PE reads with any end has
146 more than 50% inferior quality (≤ 5) bases.

147

148 **Genome survey and contig assembly**

149 The size of the hard-shelled mussel genome was estimated using the *k*-mer-based
150 method implemented in Jellyfish (version 2.3.0) with values of 51-mers [30] and
151 GenomeScope (10,000× cut-off) [31]. The *k*-mers refer to all the *k*-mer frequency

152 distributions from a read obtained through Illumina DNA sequencing. The homozygous
153 peak of the assembly was at 57× coverage and the heterozygous peak was at 28×
154 coverage (**Fig. 3a**). The assessment of genome size by *k*-mer counting suggested a
155 complete genome size of approximately 1.51 Gb (**Fig. 3a**), which is close to the final
156 assembly (1.57 Gb) and cytogenetic estimates [32]. Sequence alignment between the
157 previous assembly (1.90 Gb) [24] and the one in this study revealed considerable
158 heterozygous redundancies in the former. This kind of overestimation of genome size
159 usually occurs in fragmented assemblies, like the recently published *M.*
160 *galloprovincialis* genome [25].

161 Genome assembly from long-read data was carried out following three methods. First,
162 long reads were *de novo* assembled using the Canu (Canu, RRID:SCR_015880) v1.5
163 software with default parameters [33]; next, error correction was performed with Racon
164 v1.3.1 [34]. Then, further polishing with Illumina short-read data was conducted using
165 Pilon (Pilon, RRID:SCR_014731) v1.22 [35]. The final assembly was approximately
166 1.57 Gb in size, consisting of 6,449 contigs with an overall median length (N50) of 1.49
167 Mb, while the previously published draft genome only had an N50 of 0.66 Mb [24].
168 The present genome had a heterozygous rate of 1.39 % (also calculated by
169 GenomeScope) and an average GC content of approximately 32%.

170

171 **Anchoring of the contigs to pseudo-moleculars with Hi-C data**

172 To complete the assembly of the hard-shelled mussel genome, Hi-C technology was
173 carried out to generate information on the interactions among contigs. DNA from fresh

174 adductor muscle tissue was used to prepare a Hi-C library. This was then sequenced on
175 the Illumina NovaSeq 6000 platform, producing 249.6 Gb of reads (**Table 1**). These
176 reads were aligned to the assembled contigs using BWA (BWA, RRID:SCR_010910)
177 aligner v0.7.10-r789 [36]. Lachesis v2e27abb was applied to anchor the contigs onto
178 the linkage groups using the agglomerative hierarchical clustering method [37]. Finally,
179 2,029 contigs representing 90.9% of the total assemblies were successfully anchored to
180 14 chromosomes (**Table 2**); this number was consistent with the outputs of the
181 karyotype [38]. The unclosed gaps only occupies 0.014% of the assembly (201,500 bp),
182 which is filled with Ns (**Table 2**). The N50 of the anchored contigs was over 1.7 Mb,
183 around 1.14 times of the initial assemblies from the ONT long reads.

184

185 **Genome annotation**

186 *A de novo* repeat annotation of the hard-shelled mussel genome was carried out using
187 RepeatModeler (RepeatModeler, RRID:SCR_015027) version 1.0.11 [39] and
188 RepeatMasker (RepeatMasker, RRID:SCR_012954) version 4.0.7 [40].
189 RepeatModeler was used to construct the repeat library, which was then examined using
190 two other programs, RECON and RepeatScout (RepeatScout, RRID:SCR_014653).
191 The yielded consensus sequences were manually checked by aligning to the genes from
192 the GenBank database (nt and nr; released in October 2019) to avoid that sequences of
193 the high-copy genes are masked in following process with RepeatMasker. The final
194 repeat library consisted of 2,264 consensus sequences with the respective classification
195 information, which was used to run RepeatMasker against the genome assemblies. The

196 repetitive sequences constituted a length of 735.6 Mb, representing 47.4% of the total
197 genome length (**Supplementary Table S1**). Simple sequence repeats (SSRs) were
198 identified using Tandem Repeats Finder V 4.04. Only monomers, dimers, trimers,
199 tetramers, pentamers, and hexamers with at least four repeat units were considered. The
200 total length of the 5,324 identified SSRs was approximately 138.0 kb.

201 Conserved non-coding RNAs were predicted using the Rfam 11.0 databases. Putative
202 microRNAs (miRNAs) and ribosomal RNAs (rRNAs) were predicted using Infernal
203 (Infernal, RRID:SCR_011809) version 1.1.2 [41], and transfer RNAs (tRNAs) were
204 predicted with tRNAscan-SE (tRNAscan-SE, RRID:SCR_010835) v2.0.3. A total of
205 9,186 miRNAs, 342 rRNAs, and 1,881 tRNAs were detected (**Supplementary Table**
206 **S2**).

207 Protein-coding genes were predicted using a combined strategy of *ab initio*
208 prediction, homology-based prediction, and transcriptome-based prediction (**Fig. 2**).
209 The *ab initio* prediction was conducted using the Augustus (Augustus: Gene Prediction,
210 RRID:SCR_008417) version 3.1 [38], GlimmerHMM (GlimmerHMM,
211 RRID:SCR_002654) version 1.2 [39], and SNAP (version 2006-07-28) software [42].
212 For homology-based prediction, protein sequences of two closely related mollusk
213 species (*Modiolus philippinarum* and *Bathymodiolus platifrons*), downloaded from
214 GenBank, were aligned to the genome assemblies using Exonerate (version 2.2.0) [43].
215 In parallel, transcriptomic data from 10 tissues (GenBank SRA accession ID:
216 PRJNA578350) were assembled *de novo* using Trinity (Trinity, RRID:SCR_013048)
217 version 2.4.0 [44] and Cufflinks (Cufflinks, RRID:SCR_014597) version 2.2.1 [45].

218 The outputs of both assemblers were integrated using the Program to Assemble Spliced
219 Alignments (PASA, version 2.3.3) [46]. After merging of all of these predictions using
220 EVIDENCEModeler (v1.1.0) [46], a total of 37,478 final gene models were generated
221 (**Table 3**), a number lower than that of the previously published 42,684 gene models in
222 the draft genome [24]. Functional annotations displayed that 35,471 protein-coding
223 genes (94.6% of the 37,478 gene models) align to one or more of the InterPro (version
224 5.22-61.0) [47], GO [48], KEGG [49], Swissprot [50] and NCBI non-redundant protein
225 (NR) functional databases (**Table 4; Fig. 3b**). This information is illustrated in a
226 genome landscape map (**Fig. 3c**). Using a bidirectional BLASTp between the two
227 assemblies, we observed that a considerable heterozygous redundancies (over 20%)
228 were probably included into the previous draft assemblies (**Supplementary Table S3**),
229 which might be owing to the widespread hemizyosity and massive gene
230 presence/absence variation (PAV) [25, 51] or assembling errors.

231

232 **Phylogenetic analysis**

233 Gene clusters were identified among 12 selected genomes, namely those of
234 *Chlamys farreri* (PRJNA185465), *Pinctada fucata martensii* (GCA_002216045.1), *M.*
235 *philippinarum* (GCA_002080025.1), *Crassostrea gigas* (GCF_000297895.1), *B.*
236 *platifrons* (GCA_002080005.1), *Mizuhopecten yessoensis* (GCA_002113885.2),
237 *Penaeus vannamei* (ASM378908v1), *Pecten maximus* (GCA_902652985.1), *Scapharca*
238 (*Anadara*) *broughtonii* (PRJNA521075), *Pomacea canaliculata* (PRJNA427478),
239 *Haliotis discus hannai* (PRJNA317403), and *M. coruscus*, using OrthoMCL

240 (OrthoMCL DB: Ortholog Groups of Protein Sequences, RRID:SCR_007839) version
241 1.4 with a BLASTp cut-off value of 10^{-5} and an inflation value of 1.5 [52]. A total of
242 448 single-copy genes identified by OrthoDB were aligned and concatenated. The
243 amino acid sequences were first aligned using MUSCLE (MUSCLE,
244 RRID:SCR_011812) [53], and then further concatenated to create one supergene
245 sequence for each species and form a data matrix. The phylogenetic relationships
246 among different supergenes were then assessed using a maximum-likelihood model in
247 RAxML (RAxML, RRID:SCR_006086) version 8 [54] with the optimal substitution
248 model of PROTGAMMAJTT. The robustness of the maximum-likelihood tree was
249 assessed using the bootstrap method (100 pseudo-replicates). Furthermore, single-copy
250 orthologs and one reference divergence time on the root node obtained from the
251 TimeTree database [55] were used to calibrate the divergence dates of other nodes on
252 this phylogenetic tree using the MCMC_{TREE} tool in the PAML (PAML,
253 RRID:SCR_014932) package [56]. Visualization of phylogenetic relationships with
254 FigTree (version 1.4.3) [57] suggested that *M. coruscus* is the sister taxon to the clade
255 containing *M. philippinarum* and *B. platifrons*, with a divergence time of approximately
256 129 Mya (**Fig. 3d**).

257

258 **Whole genome re-sequencing of farmed and wild individuals**

259 Chromosome-level genomes allow re-sequencing and population genetic studies. We
260 performed a preliminary assay to detect sequence variation by sequencing two genomic
261 DNA pools of wild population and farmed population. A total of 50.4 Gb and 46.7 Gb

262 of Illumina clean reads were finally generated in farmed and wild samples, respectively.

263 Over 89% reads were aligned to the reference genome with BWA (v0.7.10-r789) [36].

264 The PCR duplicates (duplicates introduced by PCR) were removed with

265 MarkDuplicates in the Picard (Picard, RRID:SCR_006525) toolkit [58]. SNPs and

266 small indels (10 bp or less) were identified with GATK (GATK , RRID:SCR_001876)

267 version 3.7 [59] with default parameters and the addition of three extra thresholds to

268 discard unreliable items during post-filter analysis, namely: 1) any two SNPs located

269 within 5 bp from each other; 2) any two indels located within 10 bp from each other;

270 and 3) any SNPs located within 5 bp from an indel. Finally, we identified 5,733,780

271 SNPs and 1,821,690 small indels in the farmed population and 5,719,771 SNPs and

272 1,820,404 small indels in the wild population. Similar distribution patterns of SNPs and

273 indels were detected between the farmed and wild population (**Supplementary Fig. S1**)

274 when nearly 99% of the SNPs/indels were shared by both populations (**Fig. 4a**),

275 reflecting that only approximately 1% of the sequence variations were farmed

276 population specific (FPS) or wild population specific (WPS). We focused on the

277 differential variations located in the flanking regions and genic regions, between the

278 farmed and wild populations, to identify candidate genes and causal mutations related

279 to morphological traits. The software SnpEff version 2.0.5 [60] was applied to detect

280 the effect of SNPs/indels by comparing the loci of SNPs/indels with those of protein-

281 coding genes, which revealed that 59 genes carrying FPS SNPs/indels (FPSGs) and 57

282 genes carrying WPS SNPs/indels (WPSGs) underwent loss of translational start sites,

283 gain or loss of stop codons, or variants in the acceptor/donor of splicing sites. Some

284 variations were observed to cluster in farmed population (**Fig. 4b**), implicating a
285 potentially influence to morphological diversity. In addition, PAV might play a role in
286 determining phenotypic traits [25, 51], which should be included in the future re-
287 sequencing analyses.

288

289 **Chromosome synteny and evolution in bivalves**

290 To investigate the evolution of the mussel chromosomes, gene collinearity was
291 constructed by aligning the genes of the king scallop *P. maximus* to the reference
292 genomes of the blood clam *S. broughtonii*, the hard-shelled mussel *M. coruscus*, the
293 pearl oyster *P. martensii*, and the Pacific oyster *C. gigas* using MCscan (version 0.8).
294 The parameters of the MCscan alignment were set as -s, 7; k, 150; m, 250; e, $1e^{-10}$. We
295 identified 404 scallop-vs-clam, 276 scallop-vs-mussel, 159 scallop-vs-pearl-oyster, and
296 232 scallop-vs-pacific-oyster syntenic blocks, which included 10,055, 4,716, 3,636, and
297 5,009 genes of blood clam, hard-shelled mussel, pearl oyster and Pacific oyster,
298 respectively. The mean gene number per syntenic block was 21.4. King scallop and
299 blood clam had the highest gene collinearity (**Fig. 5a**), consistent with their close
300 phylogenetic relationship in the Bivalvia clade [61] (**Fig. 3d**). The chromosome synteny
301 illustrated that large-scale rearrangements are rare between scallop and mussel, but
302 frequent between scallop and oysters (**Fig. 5b–d**), as exemplified by considerable
303 structural variations between the scallop and the Pacific oyster genomes (**Fig. 5d**). The
304 identified cross-chromosome rearrangements between the scallop and mussel genomes
305 were different from those between the genomes of scallop and the two oyster species

306 (Fig. 5b–e). The scallop linkage groups (PM) 1, 5, 6, 8, 10, 16, 17, 18, and 19 were
307 syntenic to a single mussel chromosome (MC) 8, 9, 3, 4, 10, 13, 11, 12, and 14,
308 respectively. PM 2 and 15 were aligned to the same reference, MC 2; similarly, PM 3
309 and 14 aligned to MC 5, PM 4 and 7 aligned to MC 1, PM 9 and 12 aligned to MC 7,
310 and PM 11 and 13 aligned to MC 6. Comparatively, some additional chromosome
311 rearrangements occurred between scallop and the two oyster species, especially the
312 Pacific oyster. Both the Pacific oyster chromosome 9 and the pearl oyster chromosome
313 7 were predominantly syntenic to the scallop PM 15, suggesting that they might carry
314 conserved genomic regions with the same origin (Fig. 5c–e). Among all the syntenic
315 chromosomes, we did not observe any chromosome to be entirely conserved in all of
316 the bivalve genomes. Intriguingly, almost all of the chromosome rearrangements
317 between the mussel and the oyster genomes were different (Fig. 5e), implicating
318 independent chromosome fusion events. In addition, the high gene collinearity between
319 the hard-shelled mussel and another three bivalves of the Pacific oyster, blood clam and
320 pearl oyster also reflected the satisfied quality of the hard-shelled mussel assemblies
321 (Fig. 5f–h). The identification of such diverse chromosome rearrangements suggested
322 a complex evolutionary history of bivalve chromosomes.

323

324 **Metamorphosis-related transcriptome analysis**

325 To profile gene expression during development and metamorphosis in hard-
326 shelled mussels, RNA-seq analysis was conducted at five developmental stages:
327 trochophore, D-veliger, umbo, pediveliger, and juvenile (PRJNA689932). The

328 quantification of gene expression enabled the detection of 33,743 transcripts with the
329 TPM > 0 at all stages (**Supplementary Table S4**). The limma statistical method was
330 used to detect DEGs based on linear models [62]. Using the trochophore as control,
331 5,795; 6,163; 9,308; and 7,486 upregulated genes [$\log_2(\text{fold-change}) > 1$ and adjusted
332 $P < 0.05$] were identified in D-veliger, umbo, pediveliger, and juvenile larvae,
333 respectively. Functional annotation indicated that these were mainly involved in
334 “environmental information processing” (“signal transduction” and “signaling
335 molecules and interaction”) and “cellular processes” (“transport and catabolism”), in
336 agreement with the key role of signal transduction and the endocrine system in larval
337 development [17].

338 Since the ability to effectuate metamorphosis develops during the pediveliger
339 stage [17], we investigate the 774 up-regulated genes during the transition from the
340 umbo to the pediveliger stage. Functional annotation revealed that they were mainly
341 employed in a network of six related pathways: “adrenergic signaling in
342 cardiomyocytes,” “calcium signaling pathway,” “MAPK signaling pathway,” “protein
343 export,” “endocytosis,” and “catecholamine biosynthesis” (**Fig. 6a**), which have been
344 reported to be involved in settlement and metamorphosis [18, 63]. The expression of
345 most of the genes involved in these pathways increased during one or more periods
346 (**Fig. 6b**). Among them, 20 genes have been functionally identified to be associated
347 with metamorphosis (**Supplementary Table S5**) and 26 up-regulated encompassing
348 from the umbo to the pediveliger stages belonged to the categories “adrenergic
349 signaling in cardiomyocytes,” “calcium signaling pathway,” and “catecholamine

350 transport”, which was consistent with the findings of a recent proteome study on larval
351 settlement and the metamorphosis of oysters [63-66]. Although some additional
352 pathways, such as “phagosome” and “oxytocin signaling pathway”, are also detected,
353 we did not analyze them in detail because still lacking evidence on their involvement
354 in metamorphosis. In summary, the analysis of the involved pathways revealed that
355 biosynthesis, transport, and transduction of catecholamines might be critical for the
356 completion of metamorphosis.

357

358 **Assembly assessment**

359 The quality of the assembled genome was validated in terms of completeness, accuracy
360 of the assemblies, and conservation of synteny. Alignment of Illumina reads against the
361 reference genome revealed insert sizes of paired-end sequencing libraries of
362 approximately 300–350 bp and a mapping rate of over 96.7%. We assayed the genome
363 completeness using Benchmark Universal Single-Copy Orthologs (BUSCO (BUSCO,
364 RRID:SCR_015008)) v4.1.4 referencing metazoan and molluscan gene sets. In the
365 metazoan dataset, the current assemblies have 89.4% complete (of which 1.0% were
366 duplicated), 1.9% incomplete and 8.7% missing BUSCOs, corresponding to a recovery
367 of 91.3% of the entire BUSCO set. In the molluscan dataset, 85.5% complete (of which
368 1.3% were duplicated), 0.8% incomplete and 13.7% missing BUSCOs were recorded,
369 corresponding to 86.3% of the entire BUSCO set. Motifs with the characteristics of
370 telomeric repeats were detected in 23 termini of the 13 chromosomes, suggesting the
371 completeness of the assemblies (**Supplementary Table S6**). The accuracy of the

372 genome assembly was evaluated by calling sequence variants through the alignment of
373 Illumina sequencing data against the genome. Sequence alignment with the BCFtools
374 (version 1.3) [67] revealed 368,991 homozygous SNP loci, reflecting an error rate of
375 less than 0.02% in the genome assemblies. In addition, the highly conserved synteny
376 and the strict correspondence of chromosome fusion points and gene assignment
377 identified between the hard-shelled mussel and king scallop genomes (**Fig. 5b**) were
378 indicative of a high-quality assembly of the hard-shelled mussel genome, since the king
379 scallop genome is considered as the best-scaffolded genome available for bivalves [68].

380

381 **Conclusion**

382 The chromosome-level assemblies of the hard-shelled mussel genome presented here
383 is a well-assembled and annotated resource that would facilitate a wide range of
384 research in mussels, bivalves, and molluscs. The outputs of this study shed light on the
385 chromosome evolution in bivalves, resulting in the regulation of the molecular
386 pathways involved in larval metamorphosis. As one of the chromosome-level genome
387 assemblies of bivalves, this genome data set will serve as a high-quality genome
388 platform for comparative genomics at the chromosome level.

389

390 **Availability of Supporting Data and Materials**

391 All of the raw Illumina and ONT reads were deposited to NCBI Sequence Read Archive
392 and the assembled genome was deposited to GenBank, under the accession number
393 PRJNA578350. Gene expression data in different developmental stages is released

394 under the accession number PRJNA689255. The corresponding genome sequences and
395 read alignments (VCF files) are available in Figshare [69] and GigaDB [70].

396

397 **Abbreviations**

398 TPM: Transcripts per Million; GATK: Genome Analysis Tool Kit; GO: Gene Ontolog;
399 KEGG: Kyoto Encyclopedia of Genes and Genomes; AC1: adenylate cyclase 1; AC10:
400 adenylate cyclase 10; Akt: RAC serine/threonine-protein kinase; CaM: calmodulin;
401 CaMKII: calcium/calmodulin-dependent protein kinase (CaM kinase) II; CAV1:
402 caveolin 1; CAV3: caveolin 3; CREB: cyclic AMP-responsive element-binding protein;
403 DBH: dopamine beta-monoxygenase; DDC: aromatic-L-amino-acid decarboxylase;
404 DHPR: voltage-dependent calcium channel gamma-1; Epac: Rap guanine nucleotide
405 exchange factor; ERK: mitogen-activated protein kinase 1/3; Gi: guanine nucleotide-
406 binding protein G(i) subunit alpha; Gq: guanine nucleotide-binding protein G(q)
407 subunit alpha; Gs: guanine nucleotide-binding protein G(s) subunit alpha; ICER: cAMP
408 response element modulator; IKS: potassium voltage-gated channel KQT-like
409 subfamily member 1; IMP2: mitochondrial inner membrane protease subunit 2; INaK:
410 sodium/potassium-transporting ATPase subunit alpha; MAOA: monoamine oxidase A;
411 MAOB: monoamine oxidase B; MSK1: ribosomal protein S6 kinase alpha-5; NCX :
412 solute carrier family 8 (sodium/calcium exchanger); NF- κ B: nuclear factor NF-kappa-
413 B p105 subunit; NHE: solute carrier family 9 (sodium/hydrogen exchanger);
414 p38MAPK: p38 MAP kinase; PI3K: phosphatidylinositol-4,5-bisphosphate 3-kinase
415 catalytic subunit alpha/beta/delta; PKA: protein kinase A; PKC α : classical protein

416 kinase C alpha type; PLC: phosphatidylinositol phospholipase C; PP1:
417 serine/threonine-protein phosphatase PP1 catalytic subunit; TnI: Troponin I; TPM:
418 tropomyosin; TYR: tyrosinase; α -ARA: alpha-1A adrenergic receptor-like; α -ARB:
419 adrenergic receptor alpha-1B; β 2AR: adrenergic receptor beta-2.

420

421 **Competing Interests**

422 The authors declare no competing interests.

423

424 **Funding**

425 This study was supported by the National Key Research and Development Program of
426 China (2018YFD0900601), Key Program for International Science and Technology
427 Cooperation Projects of Ministry of Science and Technology of China (No.
428 2018YFD0900101), the National Natural Science Foundation of China (No. 41876159,
429 No. 41606147, No. 31802321), Key Special Project for Introduced Talents Team of
430 Southern Marine Science and Engineering Guangdong Laboratory (Guangzhou)
431 (GML2019ZD0402), the Shanghai Sailing Program (18YF1410000), China
432 Postdoctoral science foundation (2019M6614770) and Program for study on genetic
433 resources, environment and strategy of mussel culture in coast of Gouqi Island offshore.

434

435 **Authors Contributions**

436 J.L.Y., Y.L. and X.L. designed and supervised the study. K.C., J.K.X, Y.T.Z, Y.F.L.

437 collected the samples and extracted the genomic DNA and RNA. Y.L., J.L. and D.D.F.

438 performed genome assembly and bioinformatics analysis. J.L.Y., D.D.F., X.L., J.L. and

439 Y.L. wrote the original manuscript. All authors reviewed the manuscript.

440

441

442 **Figure legends**

443 **Figure 1.** Sequenced individuals and sampling sites. **a.** Pictures of the sequenced
444 individuals collected in Shengsi. A wild *M. coruscus* adult was used for genome
445 sequencing. Both wild and farmed populations were used for re-sequencing. **b.** The
446 geographic locations of the sampling sites.

447

448 **Figure 2.** Workflow of genome sequencing and annotation. The rectangles indicate the
449 steps of data treatment and the diamonds indicate output or input data.

450

451 **Figure 3.** Annotation and evolution. **a.** GenomeScope plot of the 51-mer content within
452 the hard-shelled mussel genome. Estimates of genome size and read data were shown.

453 **b.** Venn diagram indicating the number of genes that were annotated in one or more
454 databases. **c.** Genomic landscape of *M. coruscus*. The chromosomes were labeled as

455 LG01 to LG14. From the outer to the inner circle: 5, marker distribution across 14
456 chromosomes at a megabase scale; 4, gene density across the whole genome; 3, SNP

457 density; 2 and 1, number of repetitive sequences and GC content across the genome. 1–
458 5 are drawn in non-overlapping 0.1-Mb sliding windows. The length of chromosomes

459 is defined by the scale (Mb) on the outer circles. **d.** Phylogenetic tree based on protein
460 sequences from 12 metazoan genomes, namely those of *Chlamys farreri*

461 (PRJNA185465), *Pinctada fucata martensii* (GCA_002216045.1), *Modiolus*
462 *philippinarum* (GCA_002080025.1), *Crassostrea gigas* (GCF_000297895.1), *Mytilus*

463 *coruscus*, *Bathymodiolus platifrons* (GCA_002080005.1), *Mizuhopecten yessoensis*

464 (GCA_002113885.2), *Penaeus vannamei* (ASM378908v1), *Pecten maximus* (GCA
465 902652985.1), *Scapharca (Anadara) broughtonii* (PRJNA521075), *Pomacea*
466 *canaliculata* (PRJNA427478), and *Haliotis discus hannai* (PRJNA317403).

467

468 **Figure 4.** Sequence variations between farmed and wild populations. **a.** Venn diagrams
469 showing the number and distribution of indels and SNPs between the farmed and wild
470 populations. **b.** Differences in the number of SNPs on the exons of *chitobiase*. The
471 rectangles indicate the 14 exons of the *chitobiase* gene and the lines between the 14
472 rectangles indicate introns; the pink matrix represents reads from the farmed population,
473 and the blue matrix represents reads from the wild population. Bases denoted by capital
474 letters are located on exons, whereas those denoted by small letters are located on
475 introns.

476

477 **Figure 5.** Chromosome synteny. **a.** Alignment of king scallop and blood clam
478 chromosomes. **b.** Alignment of king scallop and hard-shelled mussel chromosomes. **c.**
479 Alignment of king scallop and pearl oyster chromosomes. **d.** Alignment of king scallop
480 and Pacific oyster chromosomes. **e.** Rearrangements between the chromosomes of king
481 scallop and those of four other bivalve species. The king scallop chromosomes are
482 represented by bars of different colors, and synteny and rearrangements in the
483 chromosomes of the four other bivalves are indicated by different blocks, whose colors
484 correspond to those of the reference king scallop chromosomes, the dashed lines
485 indicate the corresponding evolutionary relationship. **f.** Alignment of hard-shelled

486 mussel and blood clam chromosomes. **g.** Alignment of hard-shelled mussel and pearl
487 oyster chromosomes. **h.** Alignment of hard-shelled mussel and Pacific oyster
488 chromosomes. The king scallop linkage groups are labeled as PM 1 to 19, the blood
489 clam chromosomes as SB 1 to 19, the hard-shelled mussel chromosomes as MC 1 to
490 14, the pearl oyster chromosomes as PF 1 to 14, and the Pacific oyster chromosomes as
491 CG 1 to 10. Scale unit, Mb. **a–d, f–h.** The circularized blocks represent the
492 chromosomes of the five bivalves. Aligned homologous genes are connected by ribbons,
493 shown in different colors depending on their chromosome location.

494

495 **Figure 6.** Spatial and temporal expression of genes involved in development and
496 metamorphosis. **a.** Expression pattern of genes implied in the pathways of
497 catecholamine biosynthesis and adrenergic signaling in cardiomyocytes, according to
498 KEGG-based annotation. Red rectangles indicate upregulated genes during
499 development, red rectangles with black edge indicate upregulated genes at Pediveliger
500 stage and metamorphosis, and white rectangles denote genes that were identified during
501 KEGG analysis but whose expression did not change. Red bubbles represent the most
502 important pathways in which the upregulated genes are involved. **b.** Heatmap showing
503 the expression levels of all genes involved in the pathways of catecholamine
504 biosynthesis and adrenergic signaling in cardiomyocytes across five developmental
505 stages. These quantification results of gene expression are the averages of three
506 replicate samples.

507

508 **Table captions**

509 **Table 1.** Statistics of whole genome sequencing using Illumina and ONT

510 **Table 2.** Results of contig anchoring on pseudochromosomes using Hi-C data

511 **Table 3.** General statistics of the predicted protein-coding genes

512 **Table 4.** General statistics of gene functional annotation

513

514 **Additional Files**

515 **Supplementary Table S1.** Repetitive sequences in the hard-shelled mussel genome

516 **Supplementary Table S2.** Overview of the predicted non-coding RNAs

517 **Supplementary Table S3.** Bidirectional BLASTp between the previously published
518 gene models of the hard-shelled mussel and the predicted gene models in this study.

519 **Supplementary Table S4.** Gene expression profiles during five developmental stages

520 **Supplementary Table S5.** Genes involved in the pathways of catecholamine
521 biosynthesis and adrenergic signaling in the cardiomyocytes were reported to affect
522 metamorphosis.

523 **Supplementary Table S6.** Information of the motifs with the characteristic of telomeric
524 repeats

525 **Supplementary Figure S1.** Circles showing genome-wide SNPs and indels from the
526 farmed and wild populations. From the outer to the inner circle: first circle, marker
527 distribution across 14 pseudochromosomes at a megabase scale; green circle, SNP
528 density across the whole genome; red circle, indel density.

529

530 References

- 531 1. FAO. The state of world fisheries and aquaculture. 2018.
- 532 2. Amini S, Kolle S, Petrone L, et al. Preventing mussel adhesion using lubricant-infused
533 materials. *Science* 2017; **357**:668-673.
- 534 3. Yang JL, Li YF, Guo XP, et al. The effect of carbon nanotubes and titanium dioxide
535 incorporated in PDMS on biofilm community composition and subsequent mussel
536 plantigrade settlement. *Biofouling* 2016; **32**:763-777.
- 537 4. Yang JL, Shen PJ, Liang X, et al. Larval settlement and metamorphosis of the mussel
538 *Mytilus coruscus* in response to monospecific bacterial biofilms. *Biofouling* 2013; **29**:247-
539 259.
- 540 5. Liang X, Peng LH, Zhang S, et al. Polyurethane, epoxy resin and polydimethylsiloxane
541 altered biofilm formation and mussel settlement. *Chemosphere* 2019; **218**:599-608.
- 542 6. Odonnell MJ, George MN, Carrington E. Mussel byssus attachment weakened by ocean
543 acidification. *Nature Climate Change* 2013; **3**:587-590.
- 544 7. Ramesh K, Hu MY, Thomsen J, et al. Mussel larvae modify calcifying fluid carbonate
545 chemistry to promote calcification. *Nature Communications* 2017; **8**:1709.
- 546 8. Thomsen J, Stapp L, Haynert K, et al. Naturally acidified habitat selects for ocean
547 acidification-tolerant mussels. *Science Advances* 2017; **3**:e1602411.
- 548 9. Bitter MC, Kapsenberg L, Gattuso J, et al. Standing genetic variation fuels rapid adaptation
549 to ocean acidification. *Nature Communications* 2019; **10**:1-10.
- 550 10. Briand J. Marine antifouling laboratory bioassays: an overview of their diversity.
551 *Biofouling* 2009; **25**:297-311.
- 552 11. Petrone L, Kumar A, Sutanto CN, et al. Mussel adhesion is dictated by time-regulated
553 secretion and molecular conformation of mussel adhesive proteins. *Nature*
554 *Communications* 2015; **6**:8737-8737.
- 555 12. Zeng ZS, Guo XP, Cai XS, et al. Pyomelanin from *Pseudoalteromonas lipolytica* reduces
556 biofouling. *Microbial Biotechnology* 2017; **10**:1718-1731.
- 557 13. Murgarella M, Puiu D, Novoa B, et al. A first insight into the genome of the filter-feeder
558 mussel *Mytilus galloprovincialis*. *PLoS One* 2016; **11**:e0151561.
- 559 14. Sun J, Zhang Y, Xu T, et al. Adaptation to deep-sea chemosynthetic environments as
560 revealed by mussel genomes. *Nature Ecology and Evolution* 2017; **1**:0121.
- 561 15. Hadfield MG, Paul VG. In *Marine chemical ecology* (ed. McClintock, J.B & Baker, J.B)
562 Ch13. CRC Press, 2001.
- 563 16. Dobretsov S, Rittschof D. Love at first taste: induction of larval settlement by marine
564 microbes. *International Journal of Molecular Sciences* 2020; **21**:731.
- 565 17. Hadfield MG. Biofilms and marine invertebrate larvae: what bacteria produce that larvae
566 use to choose settlement sites. *Annual Review of Marine Science* 2011; **3**:453-470.
- 567 18. Shikuma NJ, Antoshechkin I, Medeiros JM, et al. Stepwise metamorphosis of the
568 tubeworm *Hydroides elegans* is mediated by a bacterial inducer and MAPK signaling.
569 *Proceedings of the National Academy of Sciences of the United States of America* 2016;
570 **113**:10097-10102.
- 571 19. Shikuma NJ, Pilhofer M, Weiss GL, et al. Marine tubeworm metamorphosis induced by
572 arrays of bacterial phage tail-like structures. *Science* 2014; **343**:529-533.

- 573 20. Kulikova VA, Lyashenko SA, Kolotukhina NK. Seasonal and interannual dynamics of
574 larval abundance of *Mytilus coruscus* Gould, 1861 (Bivalvia: Mytilidae) in Amursky Bay
575 (Peter the Great Bay, Sea of Japan). Russian Journal of Marine Biology 2011; **37**:342-347.
- 576 21. Li YF, Liu YZ, Chen YW, et al. Two toll-like receptors identified in the mantle of *Mytilus*
577 *coruscus* are abundant in haemocytes. Fish & Shellfish Immunology 2019; **90**:134-140.
- 578 22. Liang X, Zhang XK, Peng LH, et al. The flagellar gene regulates biofilm formation and
579 mussel larval settlement and metamorphosis. International Journal of Molecular Sciences
580 2020; **21**:710.
- 581 23. Yang JL, Li SH, Li YF, et al. Effects of neuroactive compounds, ions and organic solvents
582 on larval metamorphosis of the mussel *Mytilus coruscus*. Aquaculture 2013; **396-399**:106-
583 112.
- 584 24. Li RH, Zhang WJ, Lu JK, et al. The whole-genome sequencing and hybrid assembly of
585 *Mytilus coruscus*. Frontiers in Genetics 2020; **11**:1-6.
- 586 25. Gerdol M, Moreira R, Cruz F, et al. Massive gene presence-absence variation shapes an
587 open pan-genome in the Mediterranean mussel. Genome Biology 2020; **21**:275.
- 588 26. Li YL, Sun XQ, Hu XL, et al. Scallop genome reveals molecular adaptations to semi-sessile
589 life and neurotoxins. Nature Communications 2017; **8**:1721-1721.
- 590 27. Wang S, Zhang J, Jiao W, et al. Scallop genome provides insights into evolution of
591 bilaterian karyotype and development. Nature Ecology & Evolution 2017; **1**:0120.
- 592 28. Sokolov EP. An improved method for DNA isolation from mucopolysaccharide-rich
593 molluscan tissues. Journal of Molluscan Studies 2000; **66**:573-575.
- 594 29. Van Berkum NL, Lieberman-Aiden E, Williams L, et al. Hi-C: A method to study the three-
595 dimensional architecture of genomes. Journal of Visualized Experiments 2010; **39**:e1869.
- 596 30. Marçais G, Kingsford C. A fast, lock-free approach for efficient parallel counting of
597 occurrences of *k*-mers. Bioinformatics 2011; **27**:764-770.
- 598 31. Vurture GW, Sedlazeck FJ, Nattestad M, et al. GenomeScope: fast reference-free genome
599 profiling from short reads. Bioinformatics 2017; **33**:2202-2204.
- 600 32. Ieyama H, Kameoka O, Tan T, et al. Chromosomes and nuclear DNA contents of some
601 species in Mytilidae. Venus (Japanese Journal of Malacology) 1994; **53**:327-331.
- 602 33. Koren S, Walenz BP, Berlin K, et al. Canu: scalable and accurate long-read assembly via
603 adaptive *k*-mer weighting and repeat separation. Genome research 2017; **27**:722-736.
- 604 34. Vaser R, Sović I, Nagarajan N, et al. Fast and accurate de novo genome assembly from long
605 uncorrected reads. Genome Research 2017; **27**:737-746.
- 606 35. Walker BJ, Abeel T, Shea T, et al. Pilon: an integrated tool for comprehensive microbial
607 variant detection and genome assembly improvement. PloS One 2014; **9**:e112963.
- 608 36. Li H, Durbin R. Fast and accurate short read alignment with Burrows–Wheeler transform.
609 Bioinformatics 2009; **25**:1754-1760.
- 610 37. Burton JN, Adey A, Patwardhan RP, et al. Chromosome-scale scaffolding of de novo
611 genome assemblies based on chromatin interactions. Nature Biotechnology 2013; **31**:1119-
612 1125.
- 613 38. Zhuang BX. A preliminary study on the chromosome of marine bivalve, *Mytilus coruscus*.
614 Zoological Research 1984; **S2**.
- 615 39. Smit A, Hubley R. RepeatModeler Open-1.0. 2008:<http://www.repeatmasker.org/>.
- 616 40. Smit A, Hubley R, Green P. RepeatMasker Open-4.0. 2015:<http://www.repeatmasker.org/>.

- 617 41. Nawrocki EP, Eddy SR. Infernal 1.1: 100-fold faster RNA homology searches.
618 Bioinformatics 2013; **29**:2933-2935.
- 619 42. Korf I. Gene finding in novel genomes. BMC Bioinformatics 2004; **5**:59.
- 620 43. Slater GSC, Birney E. Automated generation of heuristics for biological sequence
621 comparison. BMC Bioinformatics 2005; **6**:31.
- 622 44. Grabherr MG, Haas BJ, Yassour M, et al. Trinity: reconstructing a full-length transcriptome
623 without a genome from RNA-Seq data. Nature Biotechnology 2011; **29**:644.
- 624 45. Trapnell C, Williams BA, Pertea G, et al. Transcript assembly and quantification by RNA-
625 Seq reveals unannotated transcripts and isoform switching during cell differentiation.
626 Nature Biotechnology 2010; **28**:511.
- 627 46. Haas BJ, Salzberg SL, Zhu W, et al. Automated eukaryotic gene structure annotation using
628 EVIDENCEModeler and the Program to Assemble Spliced Alignments. Genome Biology
629 2008; **9**:R7.
- 630 47. Zdobnov EM, Apweiler R. InterProScan—an integration platform for the signature-
631 recognition methods in InterPro. Bioinformatics 2001; **17**:847-848.
- 632 48. Ashburner M, Ball CA, Blake JA, et al. Gene ontology: tool for the unification of biology.
633 Nature Genetics 2000; **25**:25.
- 634 49. Kanehisa M, Goto S, Kawashima S, et al. The KEGG resource for deciphering the genome.
635 Nucleic Acids Research 2004; **32**:277-280.
- 636 50. Boeckmann B, Bairoch A, Apweiler R, et al. The SWISS-PROT protein knowledgebase
637 and its supplement TrEMBL in 2003. Nucleic Acids Research 2003; **31**:365-370.
- 638 51. Calcino AD, Kenny NJ, Gerdol M. Single individual structural variant detection uncovers
639 widespread hemizyosity in molluscs. bioRxiv 2020:298695.
- 640 52. Li L, Stoeckert CJ, Roos DS. OrthoMCL: identification of ortholog groups for eukaryotic
641 genomes. Genome Research 2003; **13**:2178-2189.
- 642 53. Edgar RC. MUSCLE: multiple sequence alignment with high accuracy and high throughput.
643 Nucleic Acids Research 2004; **32**:1792-1797.
- 644 54. Stamatakis A. RAxML-VI-HPC: maximum likelihood-based phylogenetic analyses with
645 thousands of taxa and mixed models. Bioinformatics 2006; **22**:2688-2690.
- 646 55. Kumar S, Stecher G, Suleski M, et al. TimeTree: a resource for timelines, timetrees, and
647 divergence times. Mol Biol Evol 2017; **34**:1812-1819.
- 648 56. Yang Z. PAML: a program package for phylogenetic analysis by maximum likelihood.
649 Computer Applications in the Biosciences 1997; **13**:555-556.
- 650 57. Rambaut A. FigTree, a graphical viewer of phylogenetic trees.
651 2007:<http://tree.bio.ed.ac.uk/software/figtree/>.
- 652 58. PicardToolkit. Broad Institute, GitHub Repository
653 2019:<http://broadinstitute.github.io/picard/>.
- 654 59. Mckenna A, Hanna M, Banks E, et al. The Genome Analysis Toolkit: A MapReduce
655 framework for analyzing next-generation DNA sequencing data. Genome Research 2010;
656 **20**:1297-1303.
- 657 60. Cingolani P, Platts AE, Wang LL, et al. A program for annotating and predicting the effects
658 of single nucleotide polymorphisms, SnpEff: SNPs in the genome of *Drosophila*
659 *melanogaster* strain w1118. Fly 2012; **6**:80-92.
- 660 61. Liu FY, Li YL, Yu HW, et al. MolluscDB: an integrated functional and evolutionary

661 genomics database for the hyper-diverse animal phylum Mollusca. *Nucleic Acids Res*
662 2020;**49**:D1556.

663 62. Smyth GK, Ritchie M, Thorne N, et al. LIMMA: linear models for microarray data. In
664 *Bioinformatics and Computational Biology Solutions Using R and Bioconductor*. Statistics
665 for Biology and Health. 2005.

666 63. Di G, Xiao X, Tong MH, et al. Proteome of larval metamorphosis induced by epinephrine
667 in the Fujian oyster *Crassostrea angulata*. *BMC Genomics* 2020; **21**:675.

668 64. Eisenhofer G, Tian H, Holmes C, et al. Tyrosinase: a developmentally specific major
669 determinant of peripheral dopamine. *The FASEB Journal* 2003; **17**:1248-1255.

670 65. Bonar DB, Coon SL, Walch M, et al. Control of oyster settlement and metamorphosis by
671 endogenous and exogenous chemical cues. *Bulletin of Marine Science* 1990; **46**:484-498.

672 66. Joyce A, Vogeler S. Molluscan bivalve settlement and metamorphosis: neuroendocrine
673 inducers and morphogenetic responses. *Aquaculture* 2018; **487**:64-82.

674 67. Narasimhan VM, Danecek P, Scally A, et al. BCFtools/RoH: a hidden Markov model
675 approach for detecting autozygosity from next-generation sequencing data. *Bioinformatics*
676 2016; **32**:1749-1751.

677 68. Kenny NJ, Mccarthy S, Dudchenko O, et al. The Gene-Rich Genome of the Scallop *Pecten*
678 *maximus*. *GigaScience* 2020;**9**:giaa037.

679 69. Feng DD. The hard-shelled mussel *Mytilus coruscus* - gene models, annotations and related
680 files of the whole genome. *Figshare* 2020:doi:10.6084/m6089.figshare.10259618.

681 70. Yang J, Feng D, Liu J, Xu J, Chen K, Li Y et al. Supporting data for “Chromosome-level
682 genome assembly of the hard-shelled mussel *Mytilus coruscus*, a widely distributed species
683 from the temperate areas of East Asia.” *GigaScience Database* 2021
684 <http://dx.doi.org/10.5524/100874>

685

686

687 **Table 1 Statistics of whole genome sequencing using Illumina and ONT**

Types	Method	Library size (bp)	Reads number	Clean data (Gb)	length (bp)	coverage (x)
Genome	Illumina	300-350	1,235,384,620	160.6	150	104×
Genome	ONT	20,000	11,108,773	246.8	30,945 (N50)	159×
Genome	Hi-C	\	832,911,978	249.6	150	161×
Transcriptome	Illumina	300-350	787,692,308	102.4	150	\

688

689 **Table 2 Results of contig anchoring on pseudochromosomes using Hi-C data**

LG	Length (bp)	Gene Number	Contig N50 length (bp)	Contig Number	Number of Gaps (bp)
LG01	141,585,364	3,535	2,274,693	122	12,100
LG02	144,576,766	3,347	3,700,000	88	8,700
LG03	99,268,963	2,454	1,068,300	196	19,500
LG04	99,542,347	2,554	894,135	225	22,400
LG05	122,084,758	3,159	2,900,000	96	9,500
LG06	102,382,230	2,442	2,078,006	106	10,500
LG07	122,148,919	2,720	3,437,001	91	9,000
LG08	101,363,610	2,456	2,665,365	138	13,700
LG09	90,511,107	2,243	1,458,983	124	12,300
LG10	94,491,177	2,295	1,062,238	172	17,100
LG11	85,619,405	1,927	619,639	249	24,800
LG12	76,129,233	1,754	767,559	180	17,900
LG13	79,962,191	1,837	2,050,444	117	11,600
LG14	63,392,598	1,391	1,000,000	125	12,400
Total	1,423,058,668	34,114	1,700,000	2,029	201,500

690 Gaps are preset at 100 Ns.

691 **Table 3** General statistics of the predicted protein-coding genes

Gene set		Number	Average transcript length (bp)	Average CDS length (bp)	Average exons per gene	Average exon length (bp)	Average intron length (bp)
<i>De novo</i>	SNAP	52,359	15,377	488	4.8	101	3,894
	GlimmerHMM	196,665	7,017	525	3.3	157	2,776
	Augustus	67,930	8,512	1,036	4.1	250	2,380
Homolog	<i>B. platifrons</i>	34,836	10,631	784	3.6	217	3,778
	<i>M. philippinarum</i>	27,088	7,174	643	2.8	227	3,568
Trans.orf/RNAseq		53,578	16,183	966	6.0	275	2,900
Final EVM models		37,478	14,735	1,290	5.9	217	2,727

692

693 **Table 4 General statistics of gene functional annotation**

Type	Number	Percentage (%)
Total	37,478	100.0
InterPro	32,821	87.6
GO	18,497	49.4
Annotated KEGG	7,625	20.3
Swissprot	16,868	45.0
NR	31,489	84.0
Annotated	35,471	94.6
Unannotated	2,007	5.4

694

a



Wild

Farmed

b

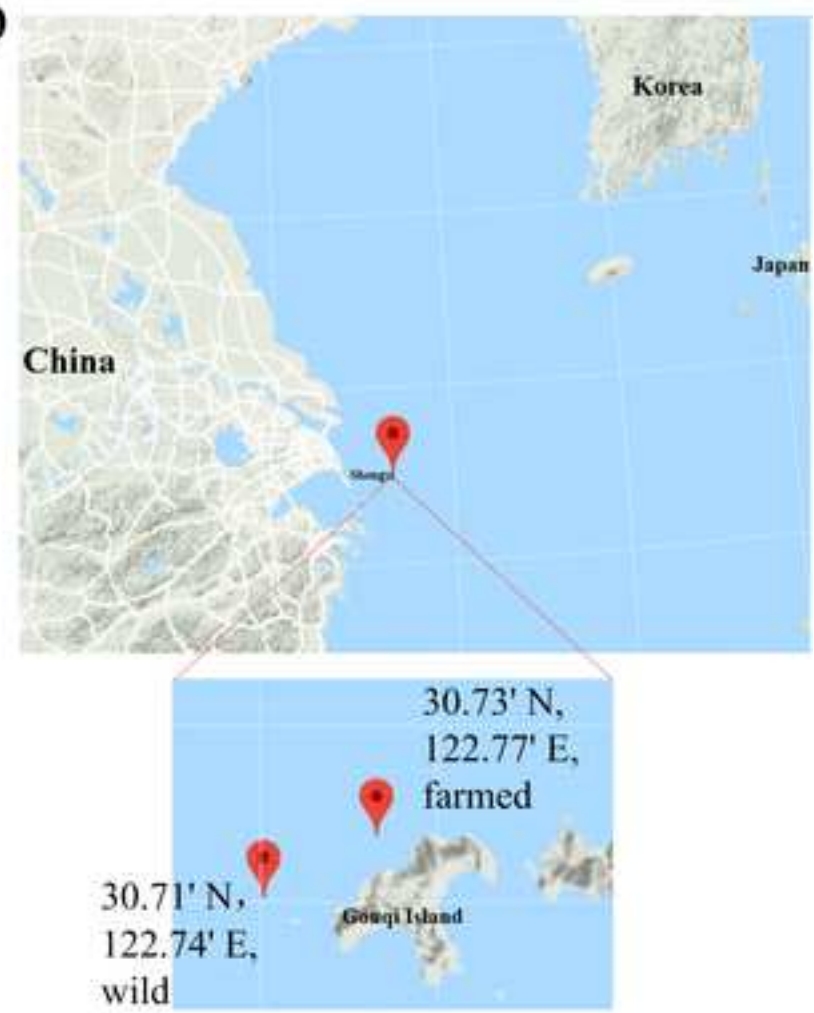


Figure 2. Workflow of genome sequencing and annotation

Click here to access/download;Figure;Figure 2. Workflow of genome sequencing and annotation.png

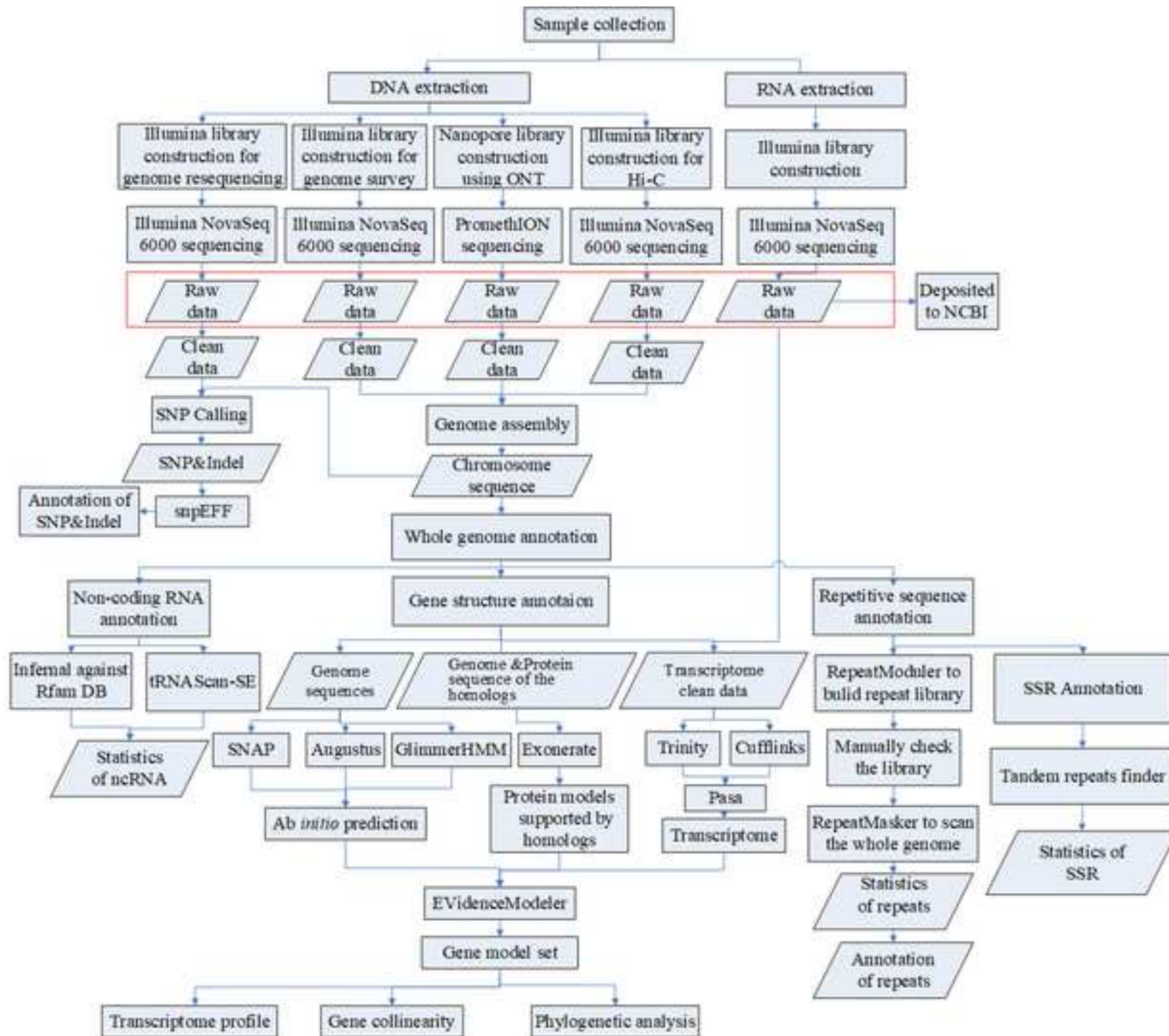
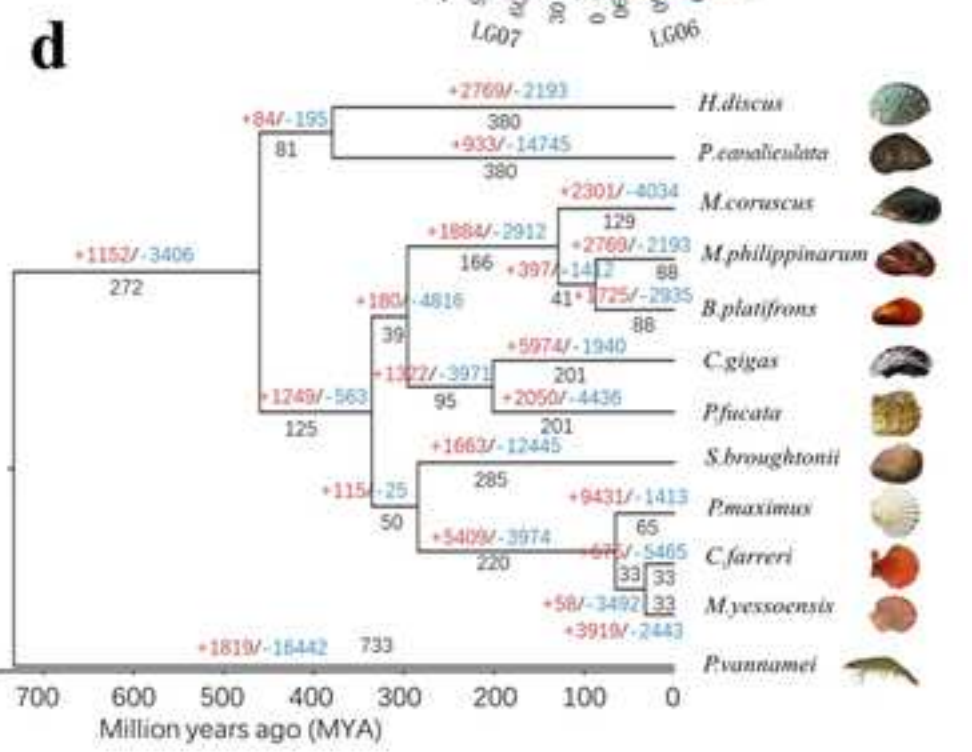
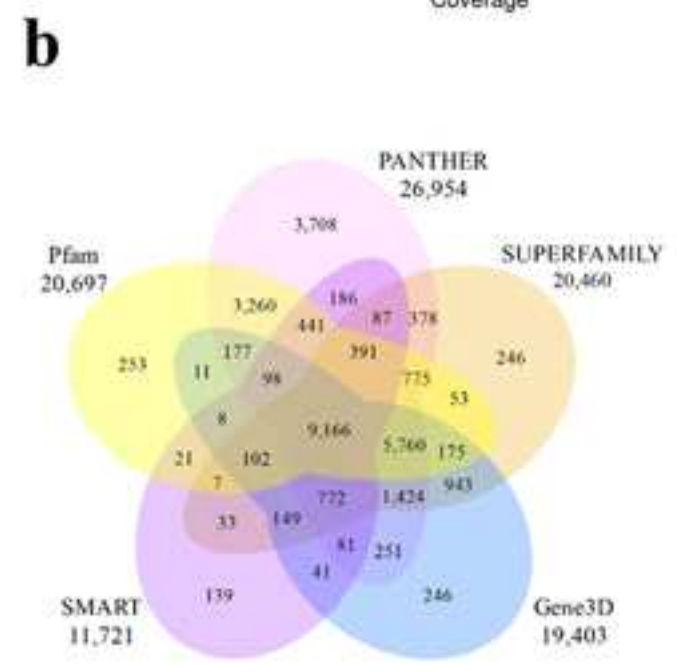
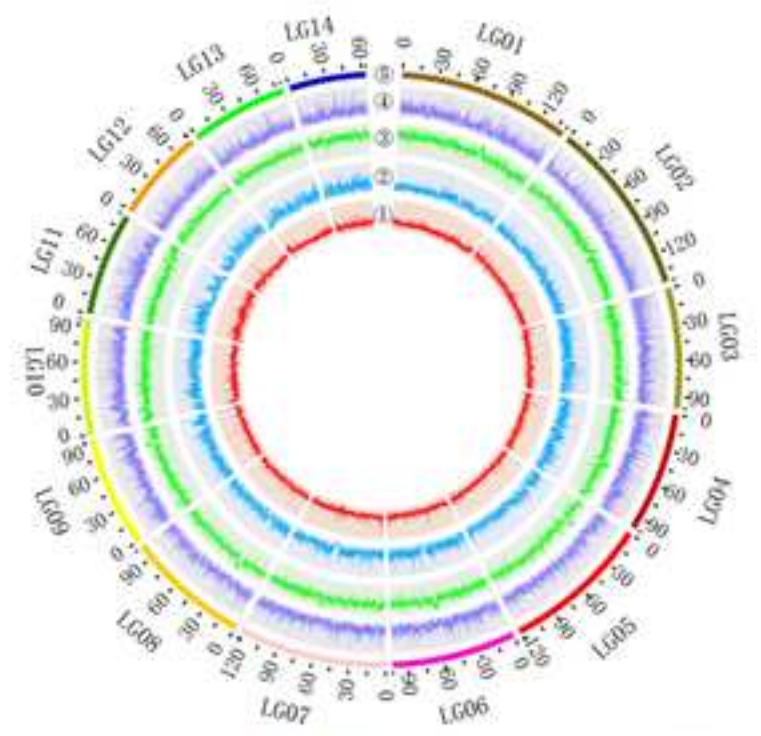
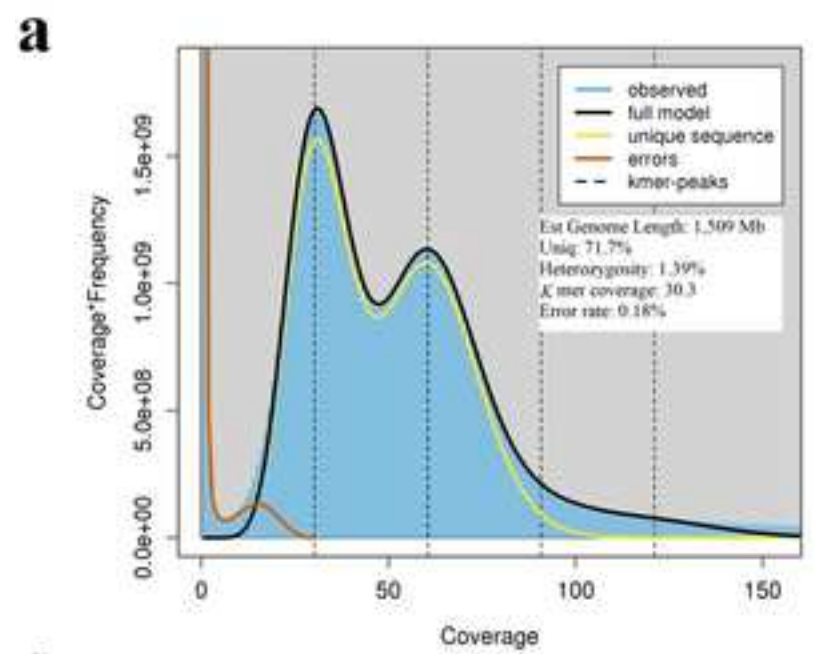
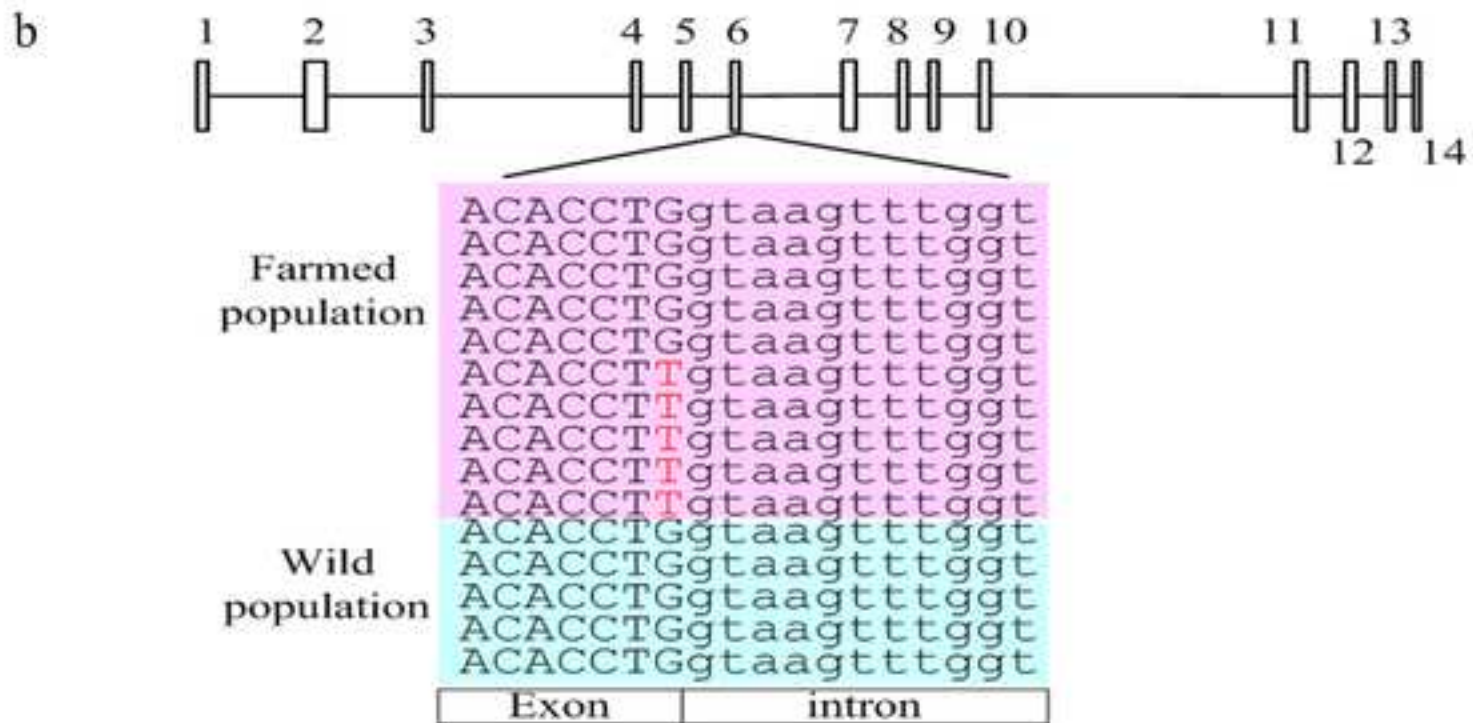
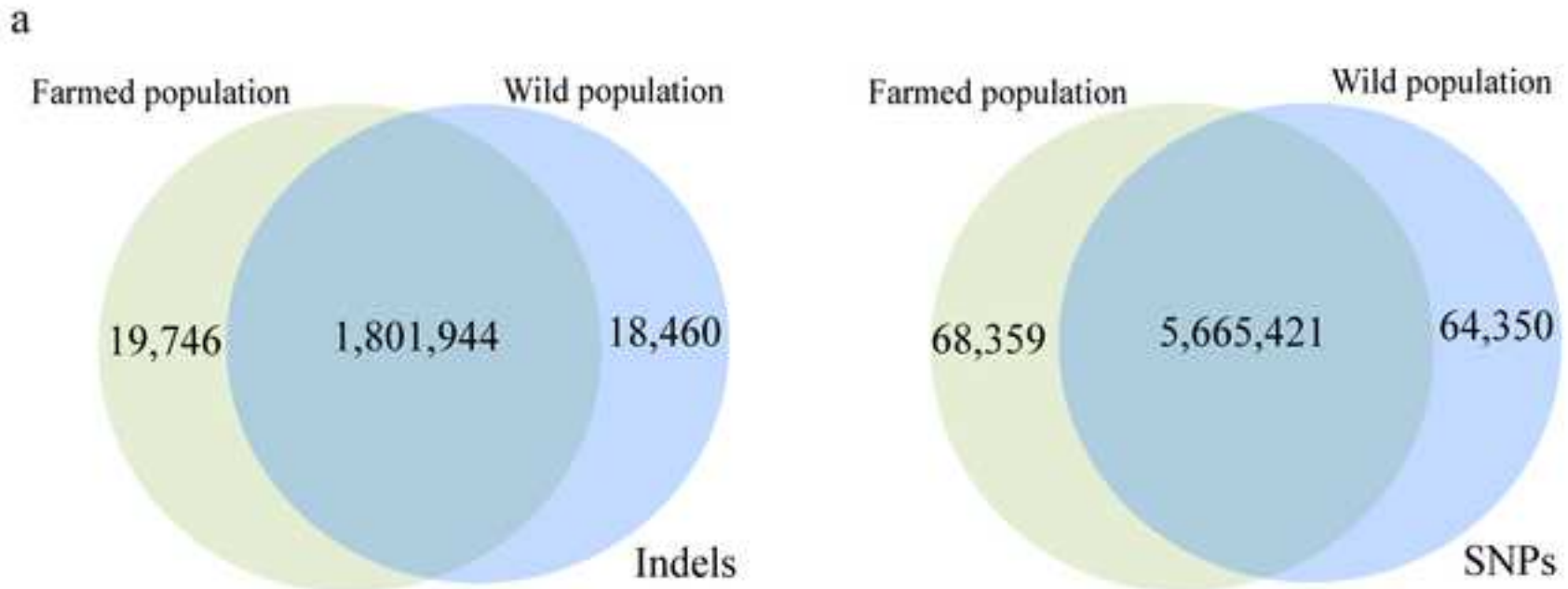


Figure 3. Annotation and evolution

[Click here to access/download;Figure;Fig3 genome annotation and evolution.jpg](#)





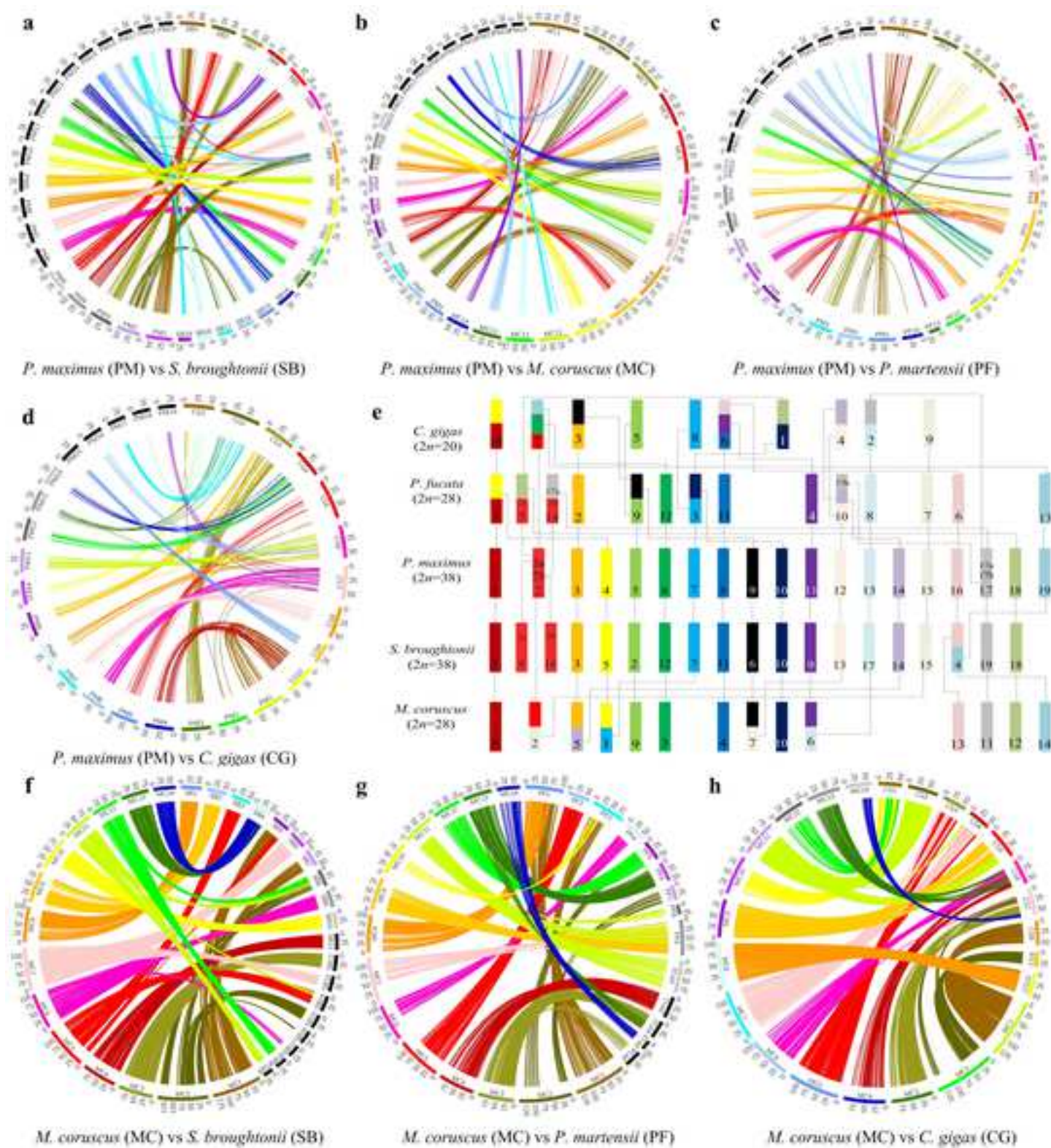
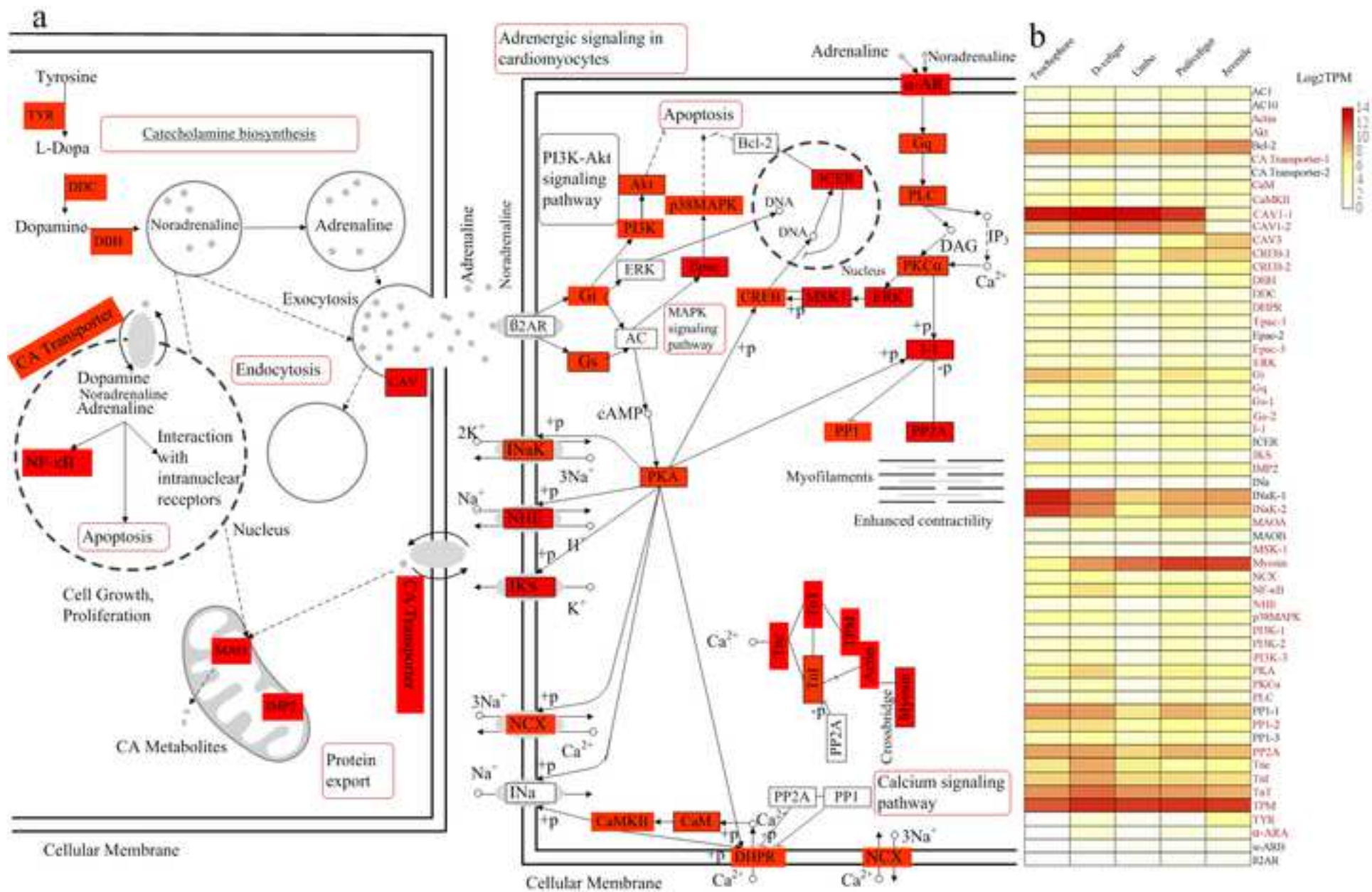


Figure 6. Spatial and temporal expression of genes involved in development and metamorphosis

[Click here to access/download;Figure;Fig6 DoapmineSynaptic.png](#)





[Click here to access/download](#)

Supplementary Material

Supplementary Table S1 Repetitive sequences.xls

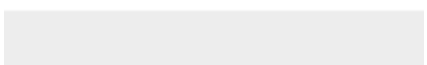
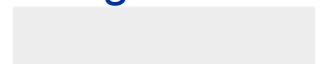


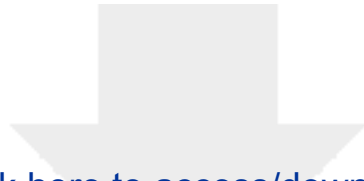


Click here to access/download

Supplementary Material

Supplementary Table S2 Overview of predicted non-coding RNAs.xls

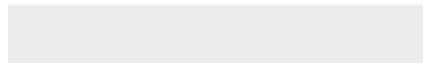




[Click here to access/download](#)

Supplementary Material

[Supplementary Table S3 Bidirectional BLASTp.docx](#)





Click here to access/download

Supplementary Material

Supplementary Table S4 The gene expression
profile.xlsx





[Click here to access/download](#)

Supplementary Material

[Supplementary Table S5 Metamorphosis.docx](#)





[Click here to access/download](#)

Supplementary Material

Supplementary Table S6 Telomeric.xlsx





[Click here to access/download](#)

Supplementary Material

[GIGA-D-20-00287R2-point-to-point_Responses22.doc](#)



GIGA-D-20-00287R2

Dear Editor Prof. Hans Zauner,

We would like to appreciate the editors and the reviewers for taking the time to review the manuscript entitled "Chromosome-level genome assembly of the hard-shelled mussel *Mytilus coruscus*, a widely distributed species from the temperate areas of East Asia ". According to the reviewers' comments, the manuscript is revised by improving the experiments and the descriptions. **All of the corresponding alterations made in the revised main text are highlighted in red.** A point-by-point letter is uploaded to address the comments. At the same time, we have performed another round of proof reading to make small corrections elsewhere in the revised main text, none of which affect substance. The related data and codes are now available in the public database.

Main alterations in the revision:

- 1) Now, we are sure that the main tables are included. And total numbers of gaps are listed in Table 2 of the revision, which describes that each gap is preset as 100 Ns (Line 693-694).
- 2) We construct the synteny between *M. coruscus* and another four reported chromosome-level genomes in the revision (Fig. 5).

Looking forward to receiving your positive reply.

Best regards.

Jin-Long Yang (jlyang@shou.edu.cn) & Ying Lu (yinglu@shou.edu.cn)

College of Fisheries and Life Science, Shanghai Ocean University, Shanghai, China